

# SCIENTIFIC REPORTS



OPEN

## A Glycyrrhetic Acid-Modified Curcumin Supramolecular Hydrogel for liver tumor targeting therapy

Guoqin Chen<sup>1,\*</sup>, Jinliang Li<sup>2,\*</sup>, Yanbin Cai<sup>3</sup>, Jie Zhan<sup>3</sup>, Jie Gao<sup>4</sup>, Mingcai Song<sup>1</sup>, Yang Shi<sup>3</sup> & Zhimou Yang<sup>3</sup>

Received: 16 November 2016

Accepted: 06 February 2017

Published: 10 March 2017

Curcumin (Cur), a phenolic anti-oxidant compound obtained from *Curcuma longa* plant, possesses a variety of therapeutic properties. However, it is suffered from its low water solubility and low bioavailability property, which seriously restricts its clinical application. In this study, we developed a glycyrrhetic acid (GA) modified curcumin supramolecular pro-gelator (GA-Cur) and a control compound Nap-Cur by replacing GA with the naphthylacetic acid (Nap). Both compounds showed good water solubility and could form supramolecular gels by disulfide bond reduction triggered by glutathione (GSH) *in vitro*. Both formed gels could sustainedly release Cur in buffer solutions. We also investigated the cytotoxicity of pro-gelators to HepG2 cells by a MTT assay and determined the cellular uptake behaviours of them by fluorescence microscopy and LC-MS. Due to the over expression of GA receptor in liver cancer cells, our pro-gelator of GA-Cur showed an enhanced cellular uptake and better inhibition capacity to liver tumor cells than Nap-Cur. Therefore, the GA-Cur could significantly inhibit HepG2 cell growth. Our study provides a novel nanomaterial for liver tumor chemotherapy.

Hepatocellular carcinoma (HCC) is one of the most common cancers in the world with a high mortality rate and few effective treatment options<sup>1,2</sup>. Surgery in combine with chemotherapy are usually the necessary and to date the main treatments for HCC. However, current chemotherapeutic agents have several shortcomings including low aqueous solubility, poor tumor selectivity and considerable side-effects to normal tissues<sup>3,4</sup>. Thus, it is very important to investigate and develop novel drug delivery systems to selectively deliver chemotherapeutic agents to liver cancer. Actually, over the past few decades, targeted drug delivery systems, especially active targeting, have shown enormous potential in cancer therapy because of their improved specificity and efficacy of anti-carcinogen and the minimized side effects<sup>5,6</sup>.

Glycyrrhetic acid (GA), a pentacyclic triterpene acid, is the main bioactive compound extracted from the herb liquorice. As a targeting ligand, GA has been demonstrated to specifically bind to liver cell membrane, because of the abundant GA receptors on hepatocyte membranes<sup>7,8</sup>. Besides, the GA receptors, identified as protein kinase C, are significantly over-expressed in HCC cells than other normal cells<sup>9,10</sup>. Therefore, GA has been widely used as a targeting ligand to functionalize nanomaterials to treat HCC, including micelles<sup>7,11,12</sup>, liposomes<sup>8,9,13</sup>, and nanospheres<sup>14–17</sup>. As results, these GA modified nanomaterials exhibited enhanced uptakes by hepatocyte and HCC cells and better inhibition effects to HCC than unmodified ones.

Curcumin (Cur), a hydrophobic polyphenol compound, is derived from the rhizomes of *Curcuma longa*. Cur has a wide range of therapeutic properties, such as anti-inflammation<sup>18</sup>, anti-oxidant<sup>19</sup>, anti-mutagenic<sup>20</sup>, and anticancer<sup>21</sup> with low or no intrinsic toxicity to healthy cells. Moreover, emerging evidences show that Cur can prevent and suppress the generation, transformation, proliferation and metastasis of many types of cancer cells including breast cancer, colon carcinoma, cervical cancer, stomach cancer, pancreatic cancer, liver cancer cells<sup>22,23</sup>. Furthermore, Cur shows great promise as a chemo-preventive and therapeutic drug in HCC, possibly because of its potent anti-angiogenic activity and pro-apoptotic properties in human HepG2 cells<sup>24</sup>. However, the clinical

<sup>1</sup>Cardiology Department of Panyu Central Hospital, Guangzhou, China; Cardiovascular Disease Institute of Panyu District, Guangzhou, Guangdong 511400, P. R. China. <sup>2</sup>Guangzhou University of Chinese Medicine, Guangzhou, Guangdong 510006, Cardiovascular Department of Panyu Central Hospital, Guangzhou, Guangdong 511400, P. R. China. <sup>3</sup>Key Laboratory of Bioactive Materials, Ministry of Education, College of Life Sciences, Nankai University, Tianjin 300071, P. R. China. <sup>4</sup>State Key Laboratory of Medicinal Chemical Biology, Nankai University, Tianjin 300071, P. R. China. \*These author contributed equally to this work. Correspondence and requests for materials should be addressed to M.S. (email: 1244919048@qq.com) Y.S. (email: snock0522@hotmail.com)

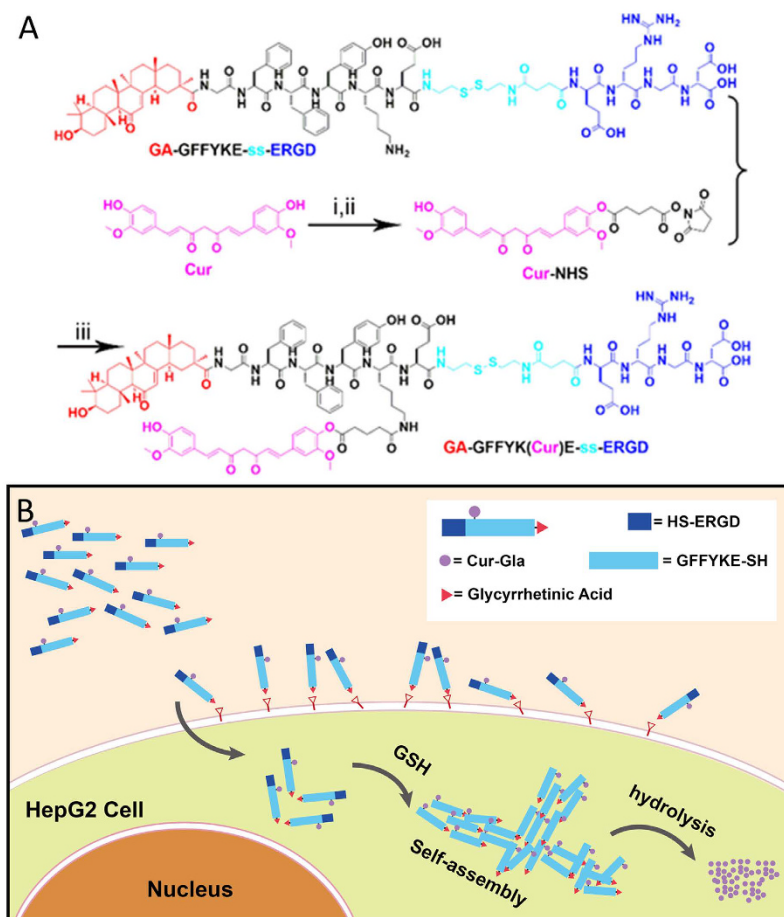


**Figure 1.** (A) Chemical structures and synthetic route for the GA-GFFYK(Cur)E-ss-ERGD (i: glutaric acid anhydride, pyridine, ii: N-hydroxy succinimide (NHS), dicyclohexylcarbodiimide (DCC), DMF, iii: DMF, DIPEA), (B) diagram to illustrate the mechanism of our compounds for tumor targeting therapy.

application of Cur remains very limited due to its extremely poor aqueous solubility ( $\approx 11$  ng/ml)<sup>25</sup> and low bio-availability<sup>26</sup>. Various approaches have been attempted to address the aforementioned problems of Cur including using biomaterials such as the polymeric micelles<sup>27–30</sup>, liposomes<sup>31–33</sup>, polymeric nanoparticles (NPs)<sup>34–36</sup>, and hydrogels<sup>37–39</sup> to deliver Cur.

As a promising biomaterial and drug carrier, supramolecular hydrogels based on short peptide and therapeutic agents have attracted extensive research interests because of the high drug loadings, sustained and responsive drug release property, good biocompatibility, ease of design and synthesis, etc<sup>40–42</sup>. Several examples of supramolecular hydrogel of therapeutic agents including Olsalazine<sup>43</sup>, Taxol<sup>44–46</sup>, Naprofen<sup>47</sup>, Camptothecin<sup>48</sup>, and Curcumin<sup>39</sup> have been rationally synthesized and reported. However, examples of *in situ* formed supramolecular hydrogels with targeting effects to cancer cells are rare. Here we designed and synthesized a glycyrrhetic acid (GA) modified curcumin supramolecular pro-gelator (GA-Cur) with a targeting effect to liver cancer cells, and we also demonstrated its improved cellular uptake and better inhibition capacity to HepG2 cells than a control compound without the targeting effect.

## Results

**Molecular design and synthesis.** We recently observed that a pro-gelator of Cur-FFE-ss-ERGD could inhibit cancer cell growth more efficiently than the corresponding gelator of Cur-FFE-s because of the enhanced cellular uptake and evenly cellular distribution of the pro-gelator<sup>39</sup>. We also demonstrated that a pro-gelator of taxol (Taxol-FFPY) exhibited a better inhibition effect to cancer cells than the corresponding gelator of Taxol-FFY because of the similar mechanism<sup>45</sup>. Xu and Liang groups also demonstrated that the intracellular formation of nanofibers or nanoparticles could significantly inhibit taxol-resistant cancer cells growth<sup>46,49</sup>. These results suggested that pro-gelators capable of forming nanomedicines within cells by intracellular catalysts might possess better inhibition capacities to cancer cells. Based on these pioneering works, we imaged that, by integrating a targeting ligand to the pro-gelator, the inhibition capacity of pro-gelators to cancer cells might be further improved.

These pioneering results and our hypothesis stimulated us to design a pro-gelator GA-GFFYK(Cur)E-ss-ERGD (GA-Cur in Fig. 1A) with a targeting ligand of GA to liver cancer cells. The pro-gelator might be converted to GA-GFFYK(Cur)E-s (GA-gelator) by disulfide bond reduction triggered by glutathione (GSH). We believed that, with the assistance of targeting ligand of GA, the pro-gelator could show a better selectivity to

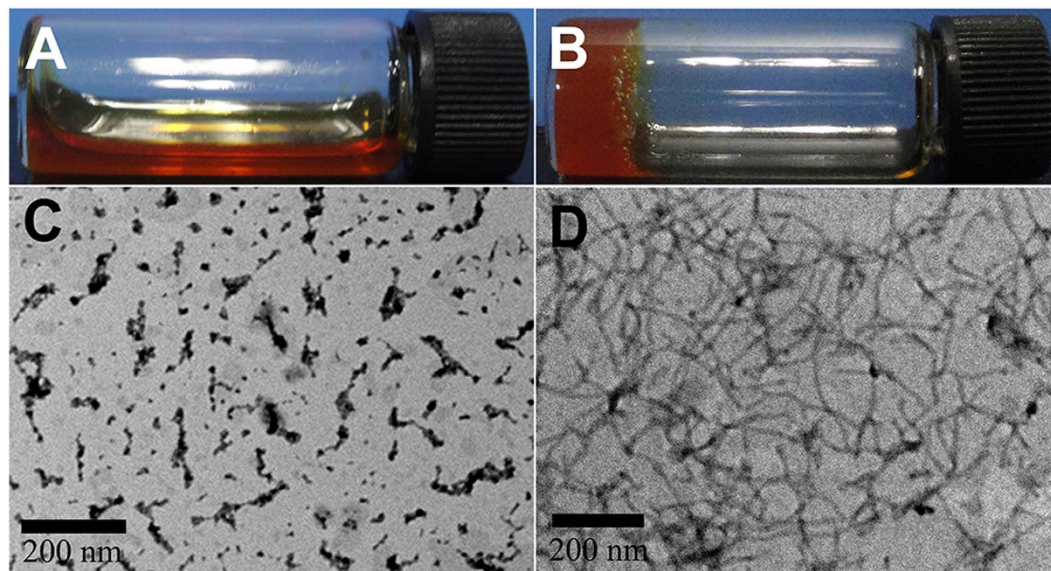


**Figure 2.** Optical images of (A) PBS solutions containing 1 wt% of the precursors (GA-Cur) and (B) the hydrogel (GA-gel) formed by treating solution in (A) with 4 equiv. of GSH, (C) transmission electron microscopy (TEM) image of the precursors (GA-cur) and (D) transmission electron microscopy (TEM) image of the hydrogel (GA-gel).

liver cancer cells than normal cells (Fig. 1B). As shown in Fig. 1A, we firstly synthesized the peptide derivative of GA-GFFYKE-ss-ERGD by standard Fmoc-solid phase peptide synthesis (SPPS), which was then used to couple with N-hydroxysuccinimide (NHS)-activated Curcumin Glutaric acid (Cur-Gla). The pure compound GA-Cur was obtained by reverse phase high performance liquid chromatography (HPLC) with a moderate yield (about 20%). We also replaced the targeting ligand of GA with naphthalene acetic acid (Nap) to make a control compound of Nap-GFFYK(Cur)E-ss-ERGD (Nap-Cur) using the similar synthetic route.

**Gelation test and characterization of hydrogels.** We therefore tested the gelation ability of the obtained two compounds. The pro-gelator GA-Cur and Nap-Cur could be well solubilized in phosphate buffer saline (PBS, pH = 7.4) at a concentration of 10 mg/mL (1 wt%, Fig. 2A; Fig. S-6A). The critical micelle concentration (CMC) of them was about 1105 and 1349  $\mu\text{g/mL}$  (Fig. S-7), respectively, which were much higher than the aqueous solubility of curcumin (11 ng/mL). After adding 4 equiv. of GSH to the solution, yellowish supramolecular hydrogels (GA-gel, Fig. 2B; Nap-gel, Fig. S-6B) could be obtained after about 1.5 h at 25  $^{\circ}\text{C}$ . The minimum gelation concentration of GA-Cur was about 0.75 wt%. The LC-MS traces clearly indicated that the pro-gelator GA-cur was converted by GSH to the gelator of GA-GFFYK(Cur)E-s (Fig. S-8). Similar gelation property was observed for Nap-cur (Fig. S-9). The hydrogels were stable and would not change the appearance for more than a month at room temperature. We then used a rheometer to characterize the resulting hydrogels obtained at 2 h time point. As shown in Fig. S-10, the value of elasticity ( $G'$ ) for the GA-gel was about 150 Pa, and that of viscosity ( $G''$ ) was about 12 Pa. The value of elasticity ( $G'$ ) and viscosity ( $G''$ ) for the Nap-gel was 1000 and 100 Pa, respectively, suggesting a better mechanical property of Nap-gel than GA-gel. We then investigated the fluorescence spectra of the precursors (GA-cur and Nap-cur) and the hydrogels (GA-gel and Nap-gel). As shown in Fig. S-11, with the amount of GSH increased, the fluorescence of GA-cur and Nap-cur quenched gradually, which was due to well-known aggregation caused quenching phenomena.

**Release profile and *In vitro* inhibition capacity.** Cur could be released from gels by ester bond hydrolysis. We then determined the release profile of Cur from both gels. As shown in Fig. 3A, both Nap-gel and GA-gel could sustainably release Cur during the 12 h experimental period, and the release speed of Cur was about 1.5 and 1.85  $\mu\text{g/mL}$  at 37  $^{\circ}\text{C}$  from GA-gel and Nap-gel, respectively. We next evaluated the inhibition capacity of the Cur, GA-Cur, Nap-Cur to both HepG2 and 3T3 cells. After incubating the cells with different compounds at a series of concentrations for 48 h, an MTT assay was performed. As shown in Fig. 3B, the Cur, GA-Cur, Nap-Cur exhibited an  $\text{IC}_{50}$  value of 26.5, 10.7, and 29.7  $\mu\text{M}$  against HepG2, respectively. For mouse fibroblast 3T3 cells, compounds of Cur, GA-Cur, and Nap-Cur showed similar  $\text{IC}_{50}$  values, which was 28.0, 29.6 and 28.7  $\mu\text{M}$ , respectively.

**Confocal microscopy and cellular uptake.** In order to understand the best inhibition capacity of GA-Cur, we obtained confocal fluorescence microscopy images of HepG2 cells treated with Cur, GA-Cur, Nap-Cur and GA + GA-Cur for 4 h. As shown in Fig. 4, we observed green fluorescence from the cytoplasm of the cells treated with different compounds. However, cells treated with GA-Cur showed the strongest green fluorescence (Fig. 4C), compared with those treated with Cur (Fig. 4A) and Nap-Cur (Fig. 4B) at the same concentration. If we firstly treating HepG2 cells with 2 equiv. of GA for 2 h and then with GA-Cur for another 4 h, the cells exhibited similar intensity of green fluorescence (Fig. 4D) to those treated with Cur and Nap-Cur. When we

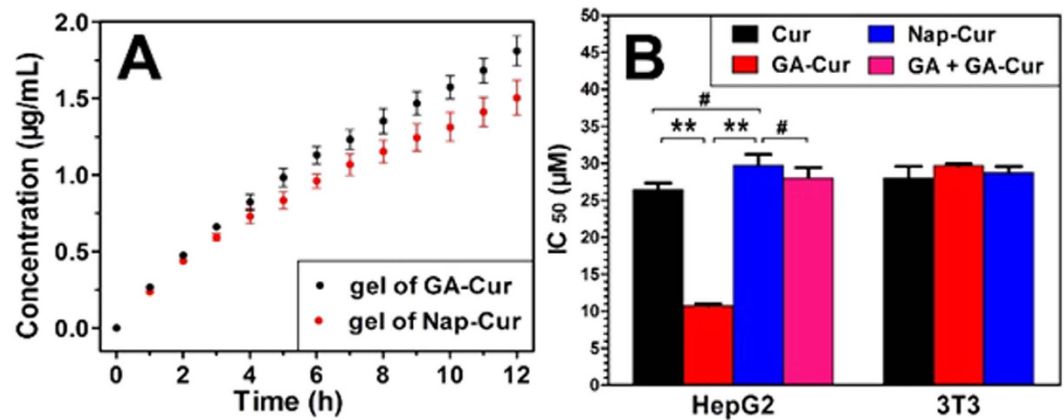


**Figure 3.** (A) Accumulative release profile at 37°C in PBS buffers (pH = 7.4) of Cur from GA-gel and Nap-gel, respectively and (B) Cytotoxicity of Cur, GA-Cur, and Nap-Cur against HepG2 and mouse NIH 3T3 cells (the IC<sub>50</sub> of GA + GA-Cur was evaluated against HepG2 cells by pre-treating cells with 2 equiv. of free GA to block the GA receptors for 2 hours and then replacing with GA-Cur for another 48 hours, #P > 0.5, \*\*P < 0.01).

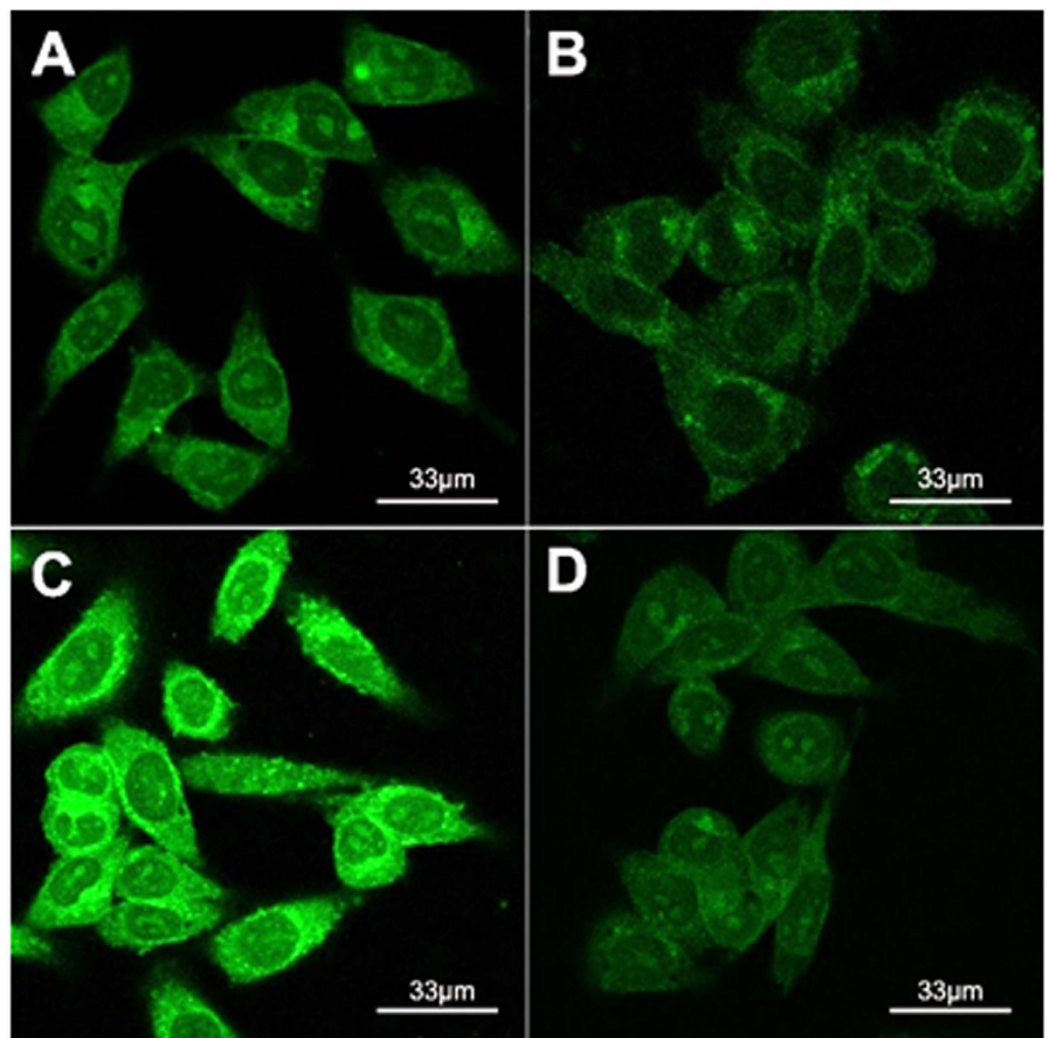


**Figure 4.** Confocal fluorescence microscopy images of HepG2 cells treated with 25 µM of (A) Cur, (B) Nap-Cur, (C) GA-Cur, and (D) GA + GA-Cur for 4 hours.

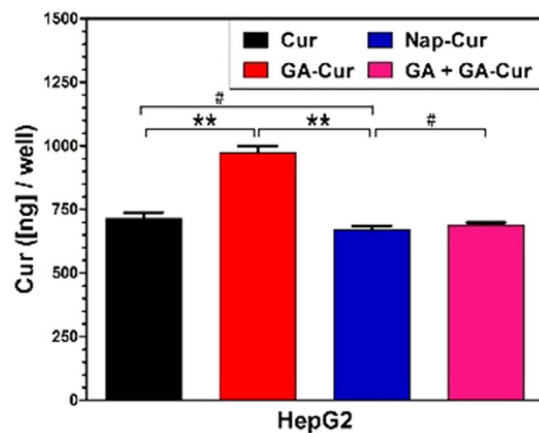


**Figure 5.** The amount of Curcumin in HepG2 cells treated with different compounds ( $\#P > 0.5$ ,  $**P < 0.01$ ).

treated the HepG2 cells with GA-cur and inhibitors (GA) together, we found that the green fluorescence of cells were also stronger than that of GA + GA-cur (Fig. S-12). These results indicated that GA-cur showed good targeting effect on HepG2 cells. We also determined the intra-cellular concentration of compounds. HepG2 cells were incubated with Cur, GA-Cur, Nap-Cur, or GA + GA-Cur (2:1) for 4 h, and then they were collected to determine the intracellular concentration of Cur. The results in Fig. 5 indicated that the intra-cellular concentration of Cur was 715, 973, 670 and 689 ng/well for Cur, GA-Cur, Nap-Cur, or GA + GA-Cur, respectively. In order to investigate whether the hydrogels have the similar inhibition capacity as pro-gelators, we took confocal fluorescence microscopy images of HepG2 cells treated with GA-gel and Nap-gel at 4 h time point containing 25  $\mu$ M curcumin. As shown in Fig. S-13, an extremely weak green fluorescence was observed in HepG2 cells. The results indicated that the cellular uptake of hydrogels were less than that of pro-gelators, which was consistent with our previous results that gels would show much lower cellular uptake than the pro-gelator<sup>50</sup>.

## Discussion

According to the rheology results (Fig. S-10), both the  $G'$  and  $G''$  of the gel showed weak frequency dependences at the frequency range from 0.1 to 100 rad/s, and the  $G'$  value of the gel was more than 10 times bigger than its corresponding  $G''$  value, suggesting the formation of a true gel. We also obtained a transmission electron microscopy (TEM) image to characterize the self-assembled nanostructures in the gel. As shown in Fig. 2C, the pro-gelator of GA-cur showed irregular short fibers in solutions, while the GA-gel exhibited uniform nanofibers with diameters of about 10 nm (Fig. 2D). The flexible nanofibers entangled with each other to form three dimensional (3D) networks for hydrogel formation. Similar to GA-Cur, the control compound Nap-Cur also formed a supramolecular hydrogel (Nap-gel) with nanofibers in the gel (Fig. S-6).

The smaller  $IC_{50}$  value (better inhibition capacity) of GA-Cur than that of Nap-Cur suggested the targeting effect of GA to HepG2 cells. If firstly treating the HepG2 cells with GA for 2 h and then with GA-Cur for another 4 h, the GA + GA-Cur group exhibited an  $IC_{50}$  value of 28  $\mu$ M, which further demonstrated the targeting effect of GA to HepG2 cells. The results of  $IC_{50}$  value and cellular uptake had clearly indicated that GA helped the accumulation of GA-Cur in HepG2 cells possibly due to the specific ligand-receptor interaction between GA and GA receptor. In order to further prove this conclusion, we performed control experiments in 3T3 cells. As shown in Fig. S-14, the fluorescent intensity of cells treated with Cur, GA-Cur, Nap-Cur, or GA + GA-Cur was similar. The intra-cellular concentration of Cur for them was also similar, which was 667, 681, 641 and 626 ng/well, respectively (Fig. S-15). These observations further demonstrated the targeting effect of GA to HepG2 cells.

**Summary.** In summary, we have developed a glycyrrhetic acid-modified curcumin supramolecular pro-gelator (GA-Cur), which could be converted to a supramolecular hydrogelator and form a hydrogel (GA-Gel) by disulfide bond reduction by GSH. Curcumin could be sustainably released from the GA-gel through ester bond hydrolysis. Compared with curcumin and Nap-Cur, GA-Cur had more potent anti-cancer efficacy and higher cellular uptake for GA positive tumor cells *in vitro*. In conclusion, GA-Cur is a promising and potential therapeutic option for hepatocellular carcinoma therapy.

## Methods

**Solid phase peptide synthesis.** Peptide derivatives of GA-GFFYKE-ss-ERGD and Nap-GFFYKE-ss-ERGD were synthesized by solid phase peptide synthesis (SPPS) using 2-chlorotrityl chloride resin and corresponding N-Fmoc protected amino acids with side chains properly protected by a tert-butyl group. The first amino acid (Fmoc-Asp(OtBu)-OH) was loaded to the resin at the C-terminal with the loading efficiency about 1.0 mmol/g. 20% piperidine in anhydrous N,N'-dimethylformamide (DMF) was used to remove Fmoc group. To couple the next Fmoc-protected amino acid, O(Benzotriazol-1-yl)-N,N,N',N'-tetramethyluronium hexafluorophosphate (HBTU) was used as the coupling reagent. The peptide chain was grown according to the standard Fmoc SPPS protocol. At the final step, glycyrrhetic acid (GA) or naphthalene acetic acid (Nap) was used. After the last coupling step, excessive reagents were removed through five times of DMF wash for 1 min, followed by five times

of washing using dichloromethane (DCM) for 1 min. To cleave the peptide derivatives from the resin, ice-cold 95% TFA (2.5% of H<sub>2</sub>O and 2.5% of TIS) was used. The reaction solution was poured into ice-cold diethylether. The resulting precipitate was centrifuged for 10 min at 4 °C at a speed of 10,000 rpm. Afterward decanting the supernatant and the solid was dried by vacuum pump.

**Synthesis of Curcumin Glutaric acid (Cur-Gla).** Curcumin (1.107 g, 3 mmol) and Glutaric acid anhydride (0.353 g, 3.1 mmol) were dissolved in pyridine (23 mL), and the resulting solution was stirred at room temperature for 7 h. The solution was removed and the crude product was re-dissolved in ethylacetate (100 mL), which was washed with 1 M HCl (30 mL) to remove pyridine. This process was repeated for three times. The ethyl acetate was removed under vacuum to get the crude product. The product was purified via silica gel column chromatography, eluted with DCM: methanol (99:1, v/v) (yield: 49.2%).

**Synthesis the pro-gelator of GA-Cur and Nap-Cur.** 0.15 mmol of peptide derivative, GA-GFFYKE-ss-ERGD or Nap-GFFYKE-ss-ERGD was reacted with 48.3 mg of Curcumin Glutaric acid N-Hydroxysuccinimide (NHS) active ester (Cur-NHS) (0.1 mmol) in the solvent of 3 mL of DMF containing 41.25  $\mu$ L of diisopropylethylamine (DIPEA, 0.25 mmol). The resulting reaction mixture was stirred at room temperature overnight. The pro-gelators were obtained by high performance liquid chromatography (HPLC) with yields of 18–25%.

**Hydrogel formation.** 3 mg of GA-Cur or Nap-Cur was dissolved in 0.25 mL phosphate buffer saline (PBS) buffer solution (pH = 7.4, adjusted by 1.5 equiv. of Na<sub>2</sub>CO<sub>3</sub>). 4equiv. of glutathione (GSH) in 0.05 mL of PBS buffer (pH = 7.4, adjusted by 3.6equiv. of Na<sub>2</sub>CO<sub>3</sub>) was added to the above solution. Gels would form after being kept at room temperature (20–25 °C) for about 1.5 hours.

**Rheology Test.** The rheology test was carried out on an AR 2000ex (TAInstrument) system. 25 mm parallel plates were used during the experiments at the gap of 500  $\mu$ m. The solution of GA-Cur or Nap-Cur (1 wt%) with 4 equiv. of GSH was directly transferred to the rheometer and waited for 2 hours for the formation of gels. The dynamic strain sweep was performed at the frequency of 1 rad/s–1. A dynamic frequency sweep at the strain of 1% was then performed.

**Transmission electron microscopy (TEM).** 15  $\mu$ L of gel was placed on a carbon-coated copper grid and incubated for 60 seconds to allow the fibers to adhere to the copper grid. The sample was then rinsed thrice with ultrapure water. The sample was then stained with a saturated uranyl acetate solution and placed in a desiccator overnight prior to analysis.

**Release profile.** A hydrogel in PBS (pH = 7.4) solution containing 1.0 wt% of pro-gelator was formed in an Eppendorf tube at 25 °C. After the gel was stable for 24 hours at 37 °C, 0.25 mL of PBS buffer solution was added on top of gels. 0.2 mL solution was taken out at the desired time point and 0.2 mL of fresh PBS was added back. We then monitored and calculated the release profile of Cur from the gel by a LCMS-20AD (Shimadzu) system. The experiment was performed at 37 °C and the results were calculated from three parallel experiments.

**Cell inhibition assay.** The IC<sub>50</sub> values of Cur, GA, GA-Cur, Nap-Cur, GA-gel, Nap-gel, GA + GA-Cur, GA + Nap-Cur were evaluated by the MTT assay. The HepG2 cells were seeded in 96-well plates at a density of 7,000 cells per well with a total medium volume of 100  $\mu$ L and then incubated for 24 hours. After removing the media, 100  $\mu$ L of the media solutions containing a serial of concentrations of compound were added to the cells. 48 hours later, we replaced the medium with fresh medium supplemented with 5  $\mu$ L MTT reagent (5 mg/mL). After another 4 hours, the medium containing MTT was removed and DMSO (100  $\mu$ L/well) was added to dissolve the formazan crystals. A microplate reader (Bio-RAD iMark™, America) was used to measure the optical density of the solution at 490 nm. Cells without any treatments were used as the control. The inhibition capacity of GA + GA-Cur or GA + Nap-Cur was evaluated against HepG2 cells by pre-treating cells with 2 equiv. of free GA to block the GA receptors for 2 hours and then replacing with GA-Cur for another 48 hours. The same experiments were performed with 3T3 cells.

**Confocal microscopy.** After being incubated for 24 h in 24-well plates at a density of 30,000 cells per-well, HepG2 cells were treated with 1 mL of DMEM solution containing 30  $\mu$ M of different compounds for 4 h. The medium was then removed and the cells were washed for three times with fresh PBS. The images were recorded under the same detected conditions (excitation wavelength = 488 nm). The samples were then dyed with DAPI for 3 min. The experiments were carried out by using a laser scanning confocal microscope. The same experiments were performed with 3T3 cells.

**Cellular uptake.** After being incubated for 24 h in 6-well plates at a density of  $2.5 \times 10^5$  cells per-well, HepG2 cells were treated with 2 mL growth medium containing 25  $\mu$ M of Cur, GA-Cur, Nap-Cur, or GA + GA-Cur, respectively. In GA + GA-Cur group, 50  $\mu$ M of GA was used to pre-treat cells for 2 hours. HepG2 cells were then rinsed for three times with PBS following with a treatment with 25  $\mu$ M of GA-Cur for another 4 hours. After 4 hours' incubation, cells were washed for three times with PBS to remove excess compounds and 500  $\mu$ L of DMSO was added to each well to dissolve compounds in cells. The solution were collected after being treated with sonication for 15 min. The amount of compounds in the cells was determined by a microplate reader excited at 488 nm. The same experiments were performed with 3T3 cells.

## References

- German, R. R. *et al.* The accuracy of cancer mortality statistics based on death certificates in the United States. *Cancer epidemiology* **35**, 126–131 (2011).
- Jemal, A. *et al.* Global cancer statistics. *CA: a cancer journal for clinicians* **61**, 69–90 (2011).
- Farokhzad, O. C. & Langer, R. Impact of nanotechnology on drug delivery. *ACS nano* **3**, 16–20 (2009).
- Shen, Y. *et al.* Prodrugs forming high drug loading multifunctional nanocapsules for intracellular cancer drug delivery. *Journal of the American Chemical Society* **132**, 4259–4265 (2010).
- Park, J. H., Saravana kumar, G., Kim, K. & Kwon, I. C. Targeted delivery of low molecular drugs using chitosan and its derivatives. *Advanced drug delivery reviews* **62**, 28–41 (2010).
- Yu, J. M., Li, Y. J., Qiu, L. Y. & Jin, Y. Polymeric nanoparticles of cholesterol-modified glycol chitosan for doxorubicin delivery: preparation and *in-vitro* and *in-vivo* characterization. *The Journal of pharmacy and pharmacology* **61**, 713–719 (2009).
- Huang, W. *et al.* Glycyrrhetic acid-modified poly(ethylene glycol)-b-poly(gamma-benzyl l-glutamate) micelles for liver targeting therapy. *Acta biomaterialia* **6**, 3927–3935 (2010).
- Mao, S. J. *et al.* Preparation, characterization and uptake by primary cultured rat hepatocytes of liposomes surface-modified with glycyrrhetic acid. *Die Pharmazie* **62**, 614–619 (2007).
- He, Z. Y. *et al.* Development of glycyrrhetic acid-modified stealth cationic liposomes for gene delivery. *International journal of pharmaceutics* **397**, 147–154 (2010).
- Il'icheva, T. N., Proniaeva, T. R., Smetannikov, A. A. & Pokrovskii, A. G. [Content of progesterone, glucocorticoid and glycyrrhizic acid receptors in normal and tumoral human breast tissue]. *Voprosy onkologii* **44**, 390–394 (1998).
- Yang, R. *et al.* Biodegradable polymer-curcumin conjugate micelles enhance the loading and delivery of low-potency curcumin. *Pharmaceutical research* **29**, 3512–3525 (2012).
- Zhang, J. *et al.* Glycyrrhetic Acid-Mediated Polymeric Drug Delivery Targeting the Acidic Microenvironment of Hepatocellular Carcinoma. *Pharmaceutical research* **32**, 3376–3390 (2015).
- Chen, J., Jiang, H., Wu, Y., Li, Y. & Gao, Y. A novel glycyrrhetic acid-modified oxaliplatin liposome for liver-targeting and *in vitro* *vivo* evaluation. *Drug design, development and therapy* **9**, 2265–2275. (2015).
- Zhang, C. *et al.* Doxorubicin-loaded glycyrrhetic acid-modified alginate nanoparticles for liver tumor chemotherapy. *Biomaterials* **33**, 2187–2196 (2012).
- Yuan, R. *et al.* Self-assembled nanoparticles of glycyrrhetic acid-modified pullulan as a novel carrier of curcumin. *Molecules* (Basel, Switzerland), **19**, 13305–13318 (2014).
- Li, J. *et al.* Synthesis, characterization, and *in vitro* evaluation of curcumin-loaded albumin nanoparticles surface-functionalized with glycyrrhetic acid. *International journal of nanomedicine* **10**, 5475–5487 (2015).
- Cheng, M. *et al.* Synthesis of glycyrrhetic acid-modified chitosan 5-fluorouracil nanoparticles and its inhibition of liver cancer characteristics *in vitro* and *in vivo*. *Marine drugs* **11**, 3517–3536 (2013).
- Srimal, R. C. & Dhawan, B. N. Pharmacology of diferuloyl methane (curcumin), a non-steroidal anti-inflammatory agent. *The Journal of pharmacy and pharmacology* **25**, 447–452 (1973).
- Kang, K. S. *et al.* Effect of intraperitoneal injection of curcumin on food intake in a goldfish model. *Journal of molecular neuroscience* **45**, 172–176 (2011).
- Polasa, K., Raghuram, T. C., Krishna, T. P. & Krishnaswamy, K. Effect of turmeric on urinary mutagens in smokers. *Mutagenesis* **7**, 107–109 (1992).
- Kuttan, R., Bhanumathy, P., Nirmala, K. & George, M. C. Potential anticancer activity of turmeric (*Curcuma longa*). *Cancer letters* **29**, 197–202 (1985).
- Kuttan, G., Kumar, K. B., Guruvayoorappan, C. & Kuttan, R. Antitumor, anti-invasion, and antimetastatic effects of curcumin. *Advances in experimental medicine and biology* **595**, 173–184 (2007).
- Shishodia, S., Chaturvedi, M. M. & Aggarwal, B. B. Role of curcumin in cancer therapy. *Current problems in cancer* **31**, 243–305, (2007).
- Yoysungnoen, P., Wirachwong, P., Bhattarakosol, P., Niimi, H. & Patumraj, S. Antiangiogenic activity of curcumin in hepatocellular carcinoma cells implanted nude mice. *Clinical hemorheology and microcirculation* **33**, 127–135 (2005).
- Kaminaga, Y. *et al.* Production of unnatural glucosides of curcumin with drastically enhanced water solubility by cell suspension cultures of *Catharanthus roseus*. *FEBS letters* **555**, 311–316 (2003).
- Anand, P., Kunnumakkara, A. B., Newman, R. A. & Aggarwal, B. B. Bioavailability of curcumin: problems and promises. *Molecular pharmaceutics* **4**, 807–818 (2007).
- Zheng, S. *et al.* Biodegradable micelles enhance the antiangioma activity of curcumin *in vitro* and *in vivo*. *International journal of nanomedicine* **11**, 2721–2736 (2016).
- Yan, T. *et al.* Effective co-delivery of doxorubicin and curcumin using a glycyrrhetic acid-modified chitosan-cystamine-poly(epsilon-caprolactone) copolymer micelle for combination cancer chemotherapy. *Colloids and surfaces. B, Biointerfaces* **145**, 526–538 (2016).
- P, R., S., James, N. R., Kumar, P. R. A. & D, K. R. Galactosylated alginate-curcumin micelles for enhanced delivery of curcumin to hepatocytes. *International journal of biological macromolecules* **86**, 1–9, (2016).
- Ni, J. *et al.* Curcumin-carboxymethyl chitosan (CNC) conjugate and CNC/LHR mixed polymeric micelles as new approaches to improve the oral absorption of P-gp substrate drugs. *Drug delivery* **1–12**, (2016).
- Roy, B. *et al.* Influence of Lipid Composition, pH, and Temperature on Physicochemical Properties of Liposomes with Curcumin as Model Drug. *Journal of oleo science* **65**, 399–411 (2016).
- Catalan-Latorre, A. *et al.* Freeze-dried eudragit-hyaluronan multicompartiment liposomes to improve the intestinal bioavailability of curcumin. *European journal of pharmaceutics and biopharmaceutics: official journal of Arbeitsgemeinschaft fur Pharmazeutische Verfahrenstechnik e.V* (2016).
- Barui, S., Saha, S., Mondal, G., Haseena, S. & Chaudhuri, A. Simultaneous delivery of doxorubicin and curcumin encapsulated in liposomes of pegylated RGDK-lipopeptide to tumor vasculature. *Biomaterials* **35**, 1643–1656 (2014).
- Muddineti, O. S. *et al.* Xanthan gum stabilized PEGylated gold nanoparticles for improved delivery of curcumin in cancer. *Nanotechnology* **27**, 325101 (2016).
- Lian, T. *et al.* Synthesis and Characterization of Curcumin-Functionalized HP-beta-CD-Modified GoldMag Nanoparticles as Drug Delivery Agents. *Journal of nanoscience and nanotechnology* **16**, 6258–6264 (2016).
- Harigae, T. *et al.* Metabolic fate of poly-(lactic-co-glycolic acid)-based curcumin nanoparticles following oral administration. *International journal of nanomedicine* **11**, 3009–3022 (2016).
- Gao, M. *et al.* Preparation and characterization of curcumin thermosensitive hydrogels for intratumoral injection treatment. *Drug development and industrial pharmacy* **40**, 1557–1564 (2014).
- Sun, Y. *et al.* Transdermal delivery of the *in situ* hydrogels of curcumin and its inclusion complexes of hydroxypropyl-beta-cyclodextrin for melanoma treatment. *International journal of pharmaceutics* **469**, 31–39 (2014).
- Yang, C. *et al.* A supramolecular hydrogelator of curcumin. *Chemical communications (Cambridge, England)* **50**, 9413–9415 (2014).
- Sun, Z. *et al.* Ferrocenoyl phenylalanine: a new strategy toward supramolecular hydrogels with multistimuli responsive properties. *Journal of the American Chemical Society* **135**, 13379–13386 (2013).

41. Ischakov, R. *et al.* Peptide-based hydrogel nanoparticles as effective drug delivery agents. *Bioorganic & Medicinal Chemistry* **21**, 3517–3522 (2013).
42. Fichman, G. & Gazit, E. Self-assembly of short peptides to form hydrogels: Design of building blocks, physical properties and technological applications. *Acta Biomaterialia* **10**, 1671–1682 (2014).
43. Li, X. *et al.* Molecular nanofibers of olsalazine form supramolecular hydrogels for reductive release of an anti-inflammatory agent. *Journal of the American Chemical Society* **132**, 17707–17709 (2010).
44. Yang, C. *et al.* Disulfide bond reduction-triggered molecular hydrogels of folic acid-Taxol conjugates. *Organic & biomolecular chemistry* **11**, 6946–6951 (2013).
45. Huang, A. *et al.* *In situ* enzymatic formation of supramolecular nanofibers for efficiently killing cancer cells. *RSC Advances* **6**, 32519–32522 (2016).
46. Gao, Y. *et al.* Enzyme-instructed molecular self-assembly confers nanofibers and a supramolecular hydrogel of taxol derivative. *Journal of the American Chemical Society* **131**, 13576–13577 (2009).
47. Li, J. *et al.* D-amino acids boost the selectivity and confer supramolecular hydrogels of a nonsteroidal anti-inflammatory drug (NSAID). *Journal of the American Chemical Society* **135**, 542–545 (2013).
48. Cheetham, A. G., Zhang, P., Lin, Y. A., Lock, L. L. & Cui, H. Supramolecular nanostructures formed by anticancer drug assembly. *Journal of the American Chemical Society* **135**, 2907–2910 (2013).
49. Li, J. *et al.* Enzyme-Instructed Intracellular Molecular Self-Assembly to Boost Activity of Cisplatin against Drug-Resistant Ovarian Cancer Cells. *Angewandte Chemie (International ed. in English)* **54**, 13307–13311 (2015).
50. Yang, C. B. *et al.* The first supramolecular hydrogelator of curcumin. *Chemical communications* **50**, 9413–9415 (2014).

## Acknowledgements

This paper is supported by the Natural Science Foundation of Guangdong Province, China (2014A030313707), Medical Scientific Research Foundation of Guangdong Province, China (A2014624) and Science & Technology Projects of Tianjin of China (15JCQNJC14300).

## Author Contributions

M. S. and Z. Y. and Y.S. designed the project and wrote the manuscript. G. C., J. L., J.G. and Y. C. did the syntheses, characterizations and cell experiments. All authors helped with manuscript preparation and revision.

## Additional Information

**Supplementary information** accompanies this paper at <http://www.nature.com/srep>

**Reprints and permission** information is available online at <http://www.nature.com/srep>

**Competing Interests:** The authors declare no competing financial interests.

**How to cite this article:** Chen, G. *et al.* A Glycyrrhetic Acid-Modified Curcumin Supramolecular Hydrogel for liver tumor targeting therapy. *Sci. Rep.* **7**, 44210; doi: 10.1038/srep44210 (2017).

**Publisher's note:** Springer Nature remains neutral with regard to jurisdictional claims in published maps and institutional affiliations.



This work is licensed under a Creative Commons Attribution 4.0 International License. The images or other third party material in this article are included in the article's Creative Commons license, unless indicated otherwise in the credit line; if the material is not included under the Creative Commons license, users will need to obtain permission from the license holder to reproduce the material. To view a copy of this license, visit <http://creativecommons.org/licenses/by/4.0/>

© The Author(s) 2017